Proceeding of the IEEE
International Conference on Robotics and Biomimetics
Dali, China, December 2019

Construction of a Production Line for Auxetic Structures Using Novel Modelling Method*

Jingru Yang, Yilun Sun, *Student Member, IEEE,* Tim C. Lueth, *Senior Member, IEEE*

Institute of Micro Technology and Medical Device Technology, Technical University of Munich
85748 Garching, Germany
yang.jingru@tum.de, yilun.sun@tum.de, tim.lueth@tum.de

***Abstract* - Auxetic materials have shown a great potential in various fields. Through additive manufacturing, auxetic structures could be easily produced. However, numrous and complex structures of them lead to a complicated modelling process. This paper presents a design, analyse, and fabrication line for auxetic materials. A novel modelling method is applied to make modelling process efficient and accurate.**

***Index Terms* – Metamaterial, Finite element method, Rapid prototyping**

I. Introduction

Since all the structures in this paper are based on auxetic materials, definition, typical models, and applications of auxetic materials will be introduced at first.

A. Auxetic Material

The concept of metamaterials includes now materials whose effective properties are generated from their internal structuring rather than the bulk behaviour of materials [1]. One example illustrating how structure controls the behaviour of mechanical metamaterials is auxetic material, that is, material with negative Poisson's ratio [2].

The property of materials to expand (contract) in directions perpendicular to the direction of compression (tension) is measured through Poisson's ratio which is denoted ν and named after Siméon Denis Poisson (1787–1840), who defined the ratio ν between transverse strain (e_t) and longitudinal strain (e_l) in the elastic loading directions as : $\nu = - e_t/e_l$ [3]. Material with Negative Poisson's ratio namely expands(compress) in the lateral direction when stretched(contracted) longitudinally [4]. Comparison of normal and auxetic materials' behaviours in tensile and compressive load is presented in Fig. 1.

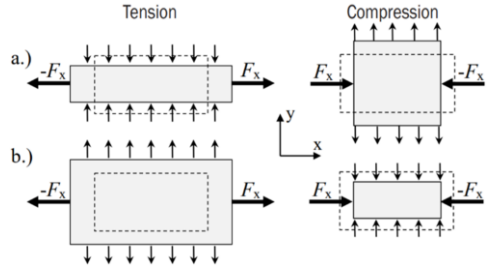

Fig. 1 Normal(a) and auxetic(b) behaviour under load [5].

B. Typical Structures and Applications of Auxetic Materials

The concept of auxetic materials has been introduced. Micro-element structures of some typical auxetic materials will be presented in this part. Also, with these micro-structures, the mechanism of auxetic behaviour could be illustrated intuitively. Finally, applications of auxetic materials will be summarised.

Dating back to 1982, the traditional cellular structure in the form of re-entrant honeycombs is firstly proposed [6]. As shown in Fig. 2, under uniaxial load, alignment of the diagonal ribs along the lateral direction of applied stretch results in the ribs aligned along the perpendicular direction moving towards outside, accordingly imparting the auxetic effect [8].

Another typical class of auxetic materials is the rotating polygonal model. Based on the assumption that the squares are non-deformable along loading directions, a novel mechanism is proposed to achieve a negative Poisson's ratio [9]. Rigid squares are connected at their vertices by hinges and auxetic behaviour is from the arrangement as presented in Fig. 3.

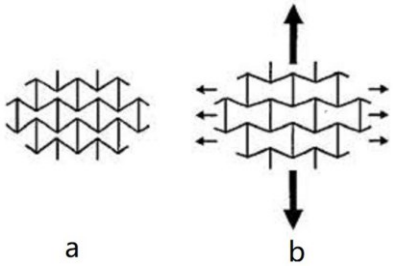

Fig. 2 The behaviour of 2D Re-entrant honeycomb: (a) Undeformed (b) Deformed [7].

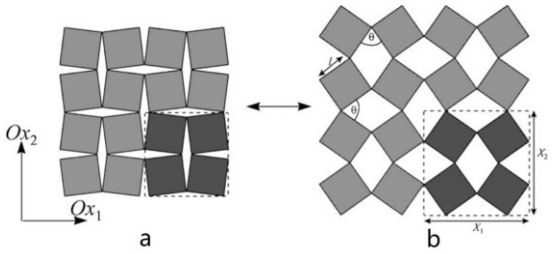

Fig. 3 The behaviour of rotating polygonal model: (a) Undeformed (b) Deformed [10].

* This work is partially supported by Department of Mechanical Engineering, Technical University of Munich

978-1-7281-6321-5/19//$31.00 ©2019 IEEE

In recent years, a configuration attracting considerable attention is the hexagonal chiral system [11]. The word 'chiral' initially means the structure lacks a centre of symmetry so that it is non-superimposable on its mirror image [12]. As shown in Fig. 4, the auxetic behaviour of hexagonal chiral is achieved by cell-wall bending [14].

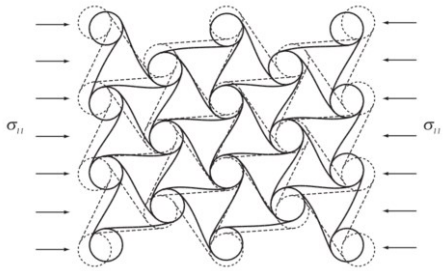

Fig. 4 Auxetic behaviour of chiral model [13].

There are still countless models, which could be regarded as extensions of variants of these models described above [15] or geometrically difficult to classify appropriately [9] such as origami-based metamaterials [16, 17] and kirigami-inspired metamaterials [18, 19].

Auxetic materials can be applied in various fields as presented in Table I.

TABLE I
APPLICATION SUMMARY OF AUXETIC MATERIALS [20]

Filed	Application and rationale
Aerospace	Vanes for engine, thermal protection, aircraft nosecones, wing panel, vibration absorber
Automotive	Bumper, cushion, thermal protection, sounds and vibration absorber parts, fastener
Biomedical	Bandage, wound pressure pad, dental floss, artificial blood vessel, artificial skin drug-release unit, ligament anchors, Surgical implants
Composite	Fibre reinforcement (because it reduces the cracking between fibre and matrix)
Military (Defence)	Helmet, bullet proof vest, knee pad, glove, protective gear (better impact property)
Sensors/actuators	Hydrophone, piezoelectric devices, various sensors
Textile (Industry)	Fibres, functional fabric, colour-change straps or fabrics, threads

II. Production Line

A. *Design in SG Library*

There are numerous structures for different auxetic materials, which results in a complicated modelling process. To make this process easy and efficient. SG Library would be used to model structures. It's a toolbox in MATLAB, developed in our institute, which aims at automatic design and manufacturing of medical robots and mechanisms [21-23]. Differences between SG Library and the conventional computer-aided design (CAD) tools are summarized as below.

At first, existing CAD tools coordinate with the traditional fabrication routines such as machining or casting well, which are suited for individual component design [24]. However, for the 3D-printing of an entire system, designers should also pay attention to fabrication factors in design process. For example, the space between different components during printing process [25].

Secondly, there are many powerful methods and toolboxes in MATLAB so that various simulations and analyses can be performed in the same environment without additional data input and output [26].

Finally, two major representation schemata are used in solid modelling which are constructive solid geometry (CSG) and boundary representation(B-rep). For 3D-printing, the most common data file is the B-rep-based STL file where a solid is represented as a list of oriented triangular facets [27]. However, most current CAD tools such as CATIA and Solidworks use CSG for modelling. Although it's possible to convert CSG model to STL file, the converted file sometimes could be imprecise and problem prone. For example, files containing self-intersecting facets. Since modelling operations tools can only be performed on the original CSG model in these CAD tools, there is no opportunity to modify the STL file in this situation. It increases design time and limits the development of additive manufacturing techniques [26].

Based on above considerations, our SG Library could directly generalize B-rep based STL file [21]. In addition, the modelling process is realised in SG-Library programmatically. Namely the complicated modelling process is implemented with simple command line. In this way, it's easy to modify and reuse the constructed models. These commands are summarized as `SGofCPLcommand`. Some common commands are shown in TABLE II.

TABLE II
TYPICAL MODELLING COMMAND IN SG-LIBRARY

Command	Operation
b x-size y-size [d]	box as rectangle or displace trapaze
c diameter diameter edges	Cylinder or ellipse as polygon
g diameter teeth-nr turn	Gear that it turned
h height z-displacement	Height of the extruded solid
sph diameter end-angle	Sphere
enter	current SG is shifted to the stack
+/add	current SG is added to stack SG

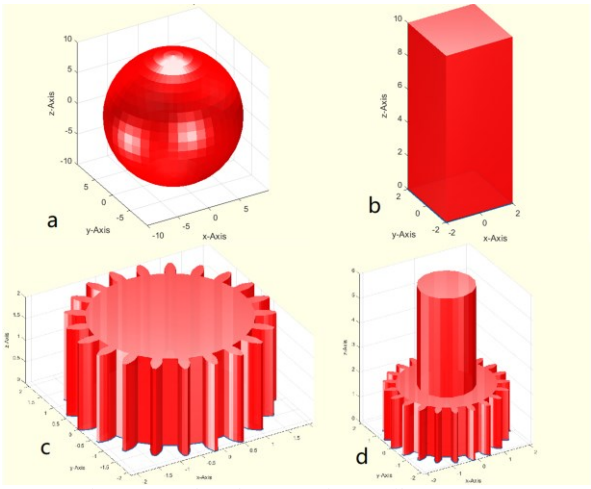

Fig. 5 Examples of structure in SG Library, a: sphere, b: cuboid, c: gear, d: gear with shaft.

Either feature parameters or a given 2D contour could be used to construct solids. Examples of structure are presented in Fig. 5. The first one is a sphere with diameter 20 mm and the corresponding code is `SGofCPLcommand ("sph 20")`. The second is cuboid extended from 4x4 mm square and it's command line is `SGofCPLcommand ("b 4, h 10")`. Through code `SGofCPLcommand ("g 4 21, h 2")`, gear with diameter 4 mm, 21 teeth, height 2 mm as shown in Fig. 5 c can be constructed. In Fig. 5 d, there is a gear with shaft, which is built through command line `SGofCPLcommand ("g 4 21, h 2, enter, c 2, h 6, +")`

Except `SGofCPLcommand`, there is an important command to build models named `SGbending`. people can bend structures to the form they need by this command. There are two examples in Fig. 6. The upper is bended on a spherical ellipsoid with code: `SGbending (SG, 5, 0, 5)` and the under is on a cylinder with code: `SGbending (SG, 5, 0)`

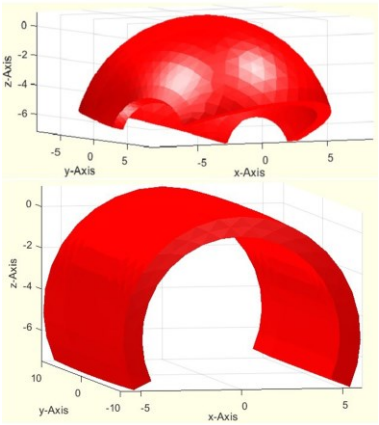

Fig. 6 Examples of bending command.

B. *Finite Element Analysis*

The next step is finite element analysis (FEA). In FEA, the von Mises stress is to be calculated. General workflow of FEA is presented in Fig. 7. Then the detail of FEA is illustrated through a simple example. We take a hemisphere as the model to be analysed, which can be easily constructed.

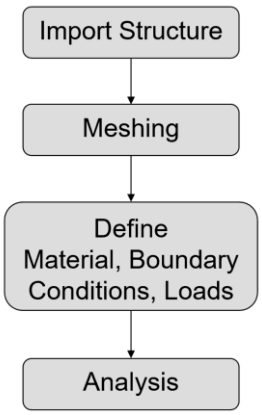

Fig. 7 The General workflow of FEA.

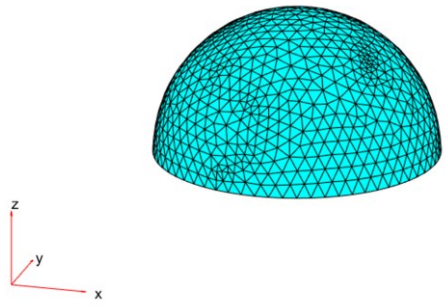

Fig. 8 The meshed hemisphere.

After model imported and meshed, people can see the meshed model, which is presented in Fig. 8. The next step is defining material through defining the material property of the model, namely Young's modulus. Then applying loading cases and boundary conditions on the given structure is necessary. Two methods to extend PDE Toolbox for specifying free-form boundary conditions have been developed in SG Library. One is Feature Surface Concept (FSC) [28], and the other is Overlapping Region Concept (ORC) [29]. Through FSC-method, the boundary conditions can be applied on regions, which with sharp boundaries divide structure into several parts. Using the ORC method, a certain space called overlapping region is occupied through constructing in SG Library, edges, or surfaces of the original geometry within the overlap region will be detected to apply the boundary conditions. Compared to the PDE Toolbox, where people can only divide the closed faces one by one and add loads to these faces. These two methods extend PDE Toolbox with significant improvement, which enable boundary conditions can be applied on appointed region with specific form. To analyse the hemisphere above, both methods are used. As shown in Fig. 9, The green region on the top of the hemisphere is a user-given overlapping region. Fixing the bottom surface and giving the overlapping region a load 1000 N, the von Mises stress of the hemisphere is calculated by the PDE Toolbox, which is presented in Fig. 10.

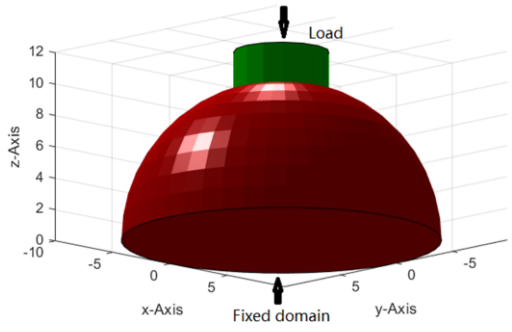

Fig. 9 Fixed domain and load domain for example model.

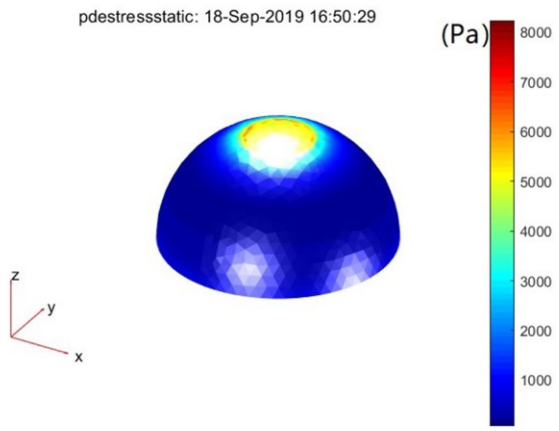

Fig. 10 FEA result of the example.

C. *Additive Manufacturing*

For manufacturing of the designed structure, layer manufacturing process: selective laser sintering (SLS) with polyamide 2200 (PA 2200) (EOS, Krailling, Germany) is used. PA 2200 is approved as biocompatible according to EN ISO 10993, which is suitable for the potential application in medical field. SLS provides the possibility to generate complex 3D parts through consolidating successive layers of powder material on top of each other [30, 31].

The mechanism of SLS is illustrated in [32, 33]: Through processing the selected areas using the thermal energy supplied by a focused laser beam, we can obtain consolidation. Each layer is scanned according to its corresponding cross section as calculated from the STL file through a beam deflection system. A powder deposition system is used to realize the deposition of successive powder layers with a typical thickness of 20 till 150 µm. There is a typical layout of SLS machine in Fig. 11.

Three steps of the production line, namely structure design, FEA and additive manufacturing with SLS machine have been presented in this section. In next part, two design examples would be introduced, also, tests would be implemented to show their properties.

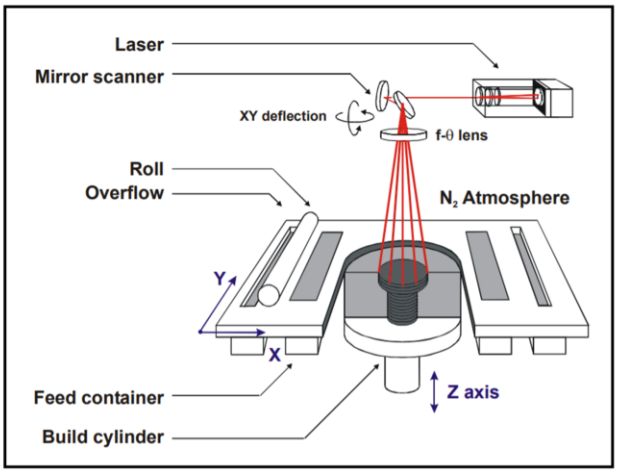

Fig. 11 Layout of a typical SLS machine [32].

III. Two Design Examples

There are two examples in this part. One is directly printed by SLS method, and the other is made of silicone rubber, which is formed by a 3D-printed mould.

A. *2D Re-entrant Structure*

As a typical auxetic structure, 2D Re-entrant structure has already been introduced in Fig. 2. To present auxetic behaviour and confirm feasibility of our production line, we choose it as the first example. Fig. 12 shows the model constructed in SG Library. The size of this model is 55 x 25 x 1 mm.

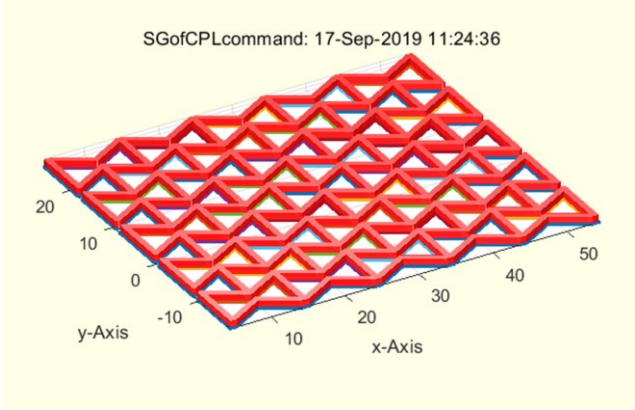

Fig. 12 2D Re-entrant structure in SG Library.

In FEA, left of this structure is fixed and load is applied on the right. Result of FEA for this structure is shown in Fig. 13. Areas of stress are presented with the help of different colours. The high stress is at the point of deformation, which is in line with the actual situation.

Finally, people can see the prototype without load in Fig. 14 a and deformed prototype in Fig. 14 b. Similar with simulation, ends of the prototype are fixed or applied load by fingers. Different with FEA showing stress distribution, deformation of protype can be seen here. The protype expands in the lateral direction when stretched longitudinally, which shows auxetic behaviour successfully.

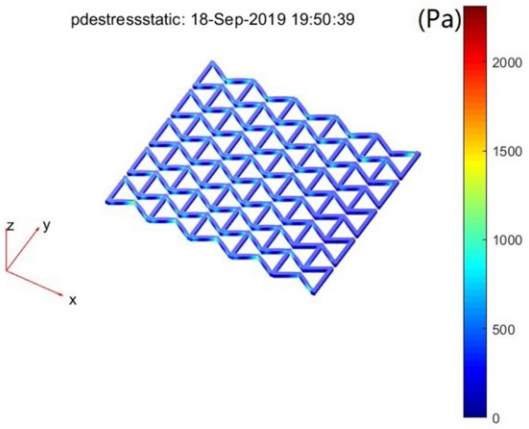

Fig. 13 FEA result of 2D Re-entrant structure.

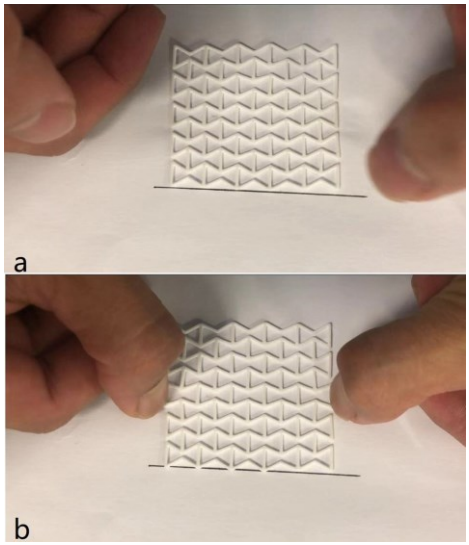

Fig. 14 Re-entrant structure without load(a) and with load (b).

B. *Auxetic Inspired Artificial Muscle*

In this part, we will introduce an auxetic-inspired, pneumatic artificial muscle. Design of the second example is inspired by the mechanism of auxetic behaviour. All the auxetic structures above are based on the deformation of small units. Designing new structure could follow this mechanism. Furthermore, a structure consisting of soft material could lead to a large deformation and it's possible to use this large deformation for actuators.

Instead of directly fabricating the artificial muscle through additive manufacturing, we build a mould firstly. More specifically, we use silicone rubber two times, each time we obtain only a half of the artificial muscle and then stick them together.

The structure details of the mould and the artificial muscle are presented in Fig. 15. The mould is shown in Fig. 15 a. Fig 15 b is the complete artificial muscle model. The artificial muscle consists of five air chambers, each of which is connected to each other as an independent deformable unit. There is a small hole in front of the muscle that can be connected to the aspirator. When the muscle is under actuation, the aspirator draws out the air from chamber leading to muscle deformation.

In Fig 16, the result of FEA for this artificial muscle can be seen. The load comes from the difference of air pressure between the air chamber and the atmosphere because the air in the chamber is drawn away by the suction device. High stress is in the upper and lower parts of the chamber because they are thinner than the left and right sides.

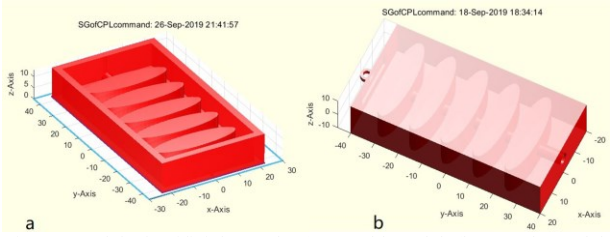

Fig. 15 Model of artificial muscle: (a) mould model, (b) muscle model.

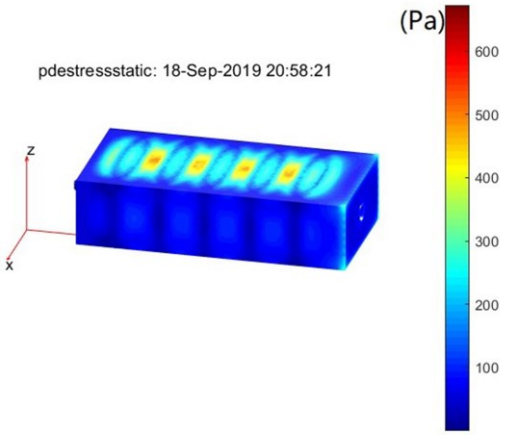

Fig. 16 FEA result of artificial muscle for stress distribution.

In Fig 17 a, there is the 3D-printed mould. It can be found that the mould is assembled in this form. It is for easy demoulding. Printing the whole mould directly could lead to tear of silicone rubber during mould release. A half of artificial muscle can be seen in Fig. 17 b. In Fig 17 c and d, people can see the comparison between the relaxed muscle and muscle under actuation. Compared with FEA result, the prototype shows its deformation and a practical actuation situation instead of stress distribution.

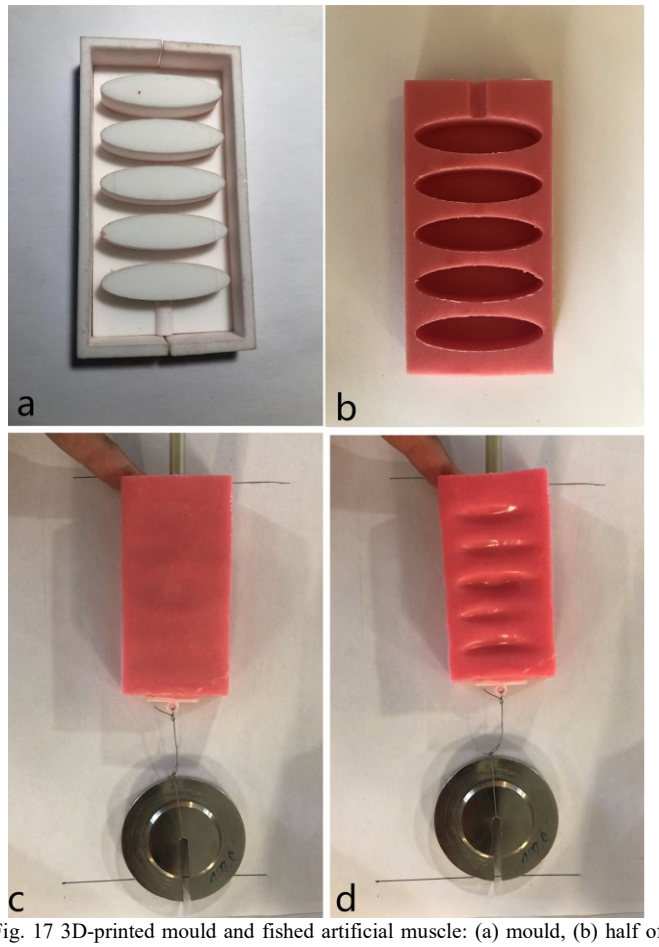

Fig. 17 3D-printed mould and fished artificial muscle: (a) mould, (b) half of artificial muscle, (c) muscle without actuation, (d) muscle with actuation.

IV. Conclusion

This paper describes a production line from structure modelling to fabrication for auxetic structures. As stated before, auxetic materials have shown great potential in various fields, but different complex structures of them make modelling process complicated. To overcome this problem, a novel modelling mothed has been applied in this production line. Our work has exactly three key advantages: Firstly, auxetic structures are constructed in SG-Library to directly generate STL-files of the auxetic structures for additive manufacturing. Secondly, complicated modelling processes are realized with short command line, which simplify modelling processes and make constructed models easily modified. Since auxetic materials consist of many same basic units, modelling with reusability could make this production line more efficient. Finally, structures could be analysed with powerful methods and toolboxes in Matlab without additional file input or output. After three processes of our production line are introduced, two typical examples have been presented. One represents the structures that can be directly produced by additive manufacturing, and the other is auxetic-inspired and formed by 3D-printed mould. Both examples' usability is proved via test. The first example presents the efficiency and convenience of our production line. The second example extends the production line's potential, which make prototype consisting of soft materials possible. In addition, SG-Library aims at automatic design of medical robots and mechanisms. Therefore, connection of medical robots and auxetic structures, construction of an automatic production line are two conceivable applications in future.

References

[1] J.-H. Lee, J. P. Singer, and E. L. Thomas, "Micro-/Nanostructured Mechanical Metamaterials," *Advanced Materials*, vol. 24, pp. 4782-4810, September 2012.

[2] K. Bertoldi, V. Vitelli, J. Christensen, and M. van Hecke, "Flexible mechanical metamaterials," *Nature Reviews Materials*, vol. 2, no. 17066, pp. 1-11, November 2017.

[3] S. D. Poisson. "Note sur l'extension des fils et des plaques elastiques," *Ann. Chim. Phys*, pp. 384-385, 1827.

[4] A. Alderson, K. L. Alderson, "Auxetic materials," *Journal of Aerospace Engineering*, vol. 221, pp. 565-575, April 2007.

[5] N. Novak, M. Vesenjak, and Z. Ren, "Auxetic Cellular Materials - a Review," *Strojniški vestnik - Journal of Mechanical Engineering*, pp. 485-493, 2016.

[6] L. J. Gibson, M. F. Ashby, G. S. Schajer and C. I. Robertson, "The mechanics of two-dimensional cellular materials," *P ROY SOC A-MATH PHY*, vol. 382, July 1982.

[7] Y. Liu and H. Hu, "A review on auxetic structures and polymeric materials," *Scientific Research and Essays*, vol. 5, pp. 1052-1063, May 2010.

[8] K. E. Evans., A. Alderson, and F. R. Christian, "Auxetic two-dimensional polymer networks. An example of tailoring geometry for specific mechanical properties," *Chem. Soc. Faraday Trans*, pp. 2671-2680, 1995.

[9] X. Ren, R. Das, P. Tran, T. D. Ngo, and Y. M. Xie, "Auxetic metamaterials and structures: a review," *Smart Materials and Structures*, January 2018.

[10] J. N. Grima and K. E. Evans "Auxetic behavior from rotating squares," Journal of Materials Science Letters, vol. 19, pp. 1563–1565, September 2000.

[11] J. N. Grima, R. Gatt, and P.-S. Farrugia "On the properties of auxetic meta-tetrachiral structures," *ßasic solid state physics*, vol. 245, pp. 511-520, March 2008.

[12] R. Lakes, "Deformation mechanisms in negative Poisson's ratio materials: structural aspects," *Journal of Materials Science*, vol 26, pp. 2287–2292, May 1991.

[13] A. Spadoni and M. Ruzzene, "Elasto-static micropolar behavior of a chiral auxetic lattice," *Journal of the Mechanics and Physics of Solids*, vol 60, pp. 156-171, January 2012.

[14] L. J. Gibson and M. F. Ashby, *Cellular Solids: Structure and Properties*, 2nd ed, Cambridge university press, 1997.

[15] J. N. Grima and R. Gatt, "Perforated Sheets Exhibiting Negative Poisson's Ratios," *Advanced engineering materials*, vol 12, pp. 460-464, June 2010.

[16] Z. Y. Wei, Z. V. Guo, L. Dudte, H. Y. Liang, and L. Mahadevan, "Geometric Mechanics of Periodic Pleated Origami," *Phys. Rev. Lett*, vol. 110, May 2013.

[17] C. Lv, D. Krishnaraju, G. Konjevod, H. Yu and H. Jiang, "Origami based Mechanical Metamaterials," *Scientific Reports*, no. 5979(2014), August 2014.

[18] R. Gatt, et al, "Hierarchical Auxetic Mechanical Metamaterials," *Scientific Reports*, no. 8395(2015), February 2015.

[19] Y. Cho, et al, "Engineering the shape and structure of materials by fractal cut," *PNAS*, pp. 17390-17395, December 2014.

[20] Y. Prawoto "Seeing auxetic materials from the mechanics point of view: A structural review," *Computational Materials Science*, pp. 140-153, 2012.

[21] T. C. Lueth and F. Irlinger, "Berechnete Erzeugung von Dreidimensionalen Oberflächenmodellen Im STL-Format Aus Der Beschreibung Planarer Mechanismen Für Die Generative Fertigung Durch Selektives Lasersintern," *11. Kolloquium Getriebetechnik*, pp. 1-18, 2013.

[22] T. C. Lueth, "SG-Library: Entwicklung Einer Konstruktiven MATLAB-Toolbox Zur Räumlichen Modellierung von Körpern, Gelenken Und Getrieben," *11. Kolloquium Getriebetechnik*, pp. 183–203, 2015.

[23] T. C. Lueth and F. Irlinger, "Automatische Generierung von Simscape Multibody Modellen Auf Der Grundlage von Gelenkgetrieben Mit Der Matlab-Toolbox SG-Library," *12. Kolloquium Getriebetechnik*, 2017.

[24] J. Hiller and H. Lipson, "Automatic Design and Manufacture of Soft Robots," *IEEE TRANSACTIONS ON ROBOTICS*, vol. 28, no. 2 April 2012.

[25] M. Alam, C. Mavroidis, N. Langrana, and P. Bidaud, "Mechanism Design Using Rapid Prototyping," *Tenth world congress on the theory of machines and mechanisms*, June 1999.

[26] Y. Sun, L. Xu, J. Yang, T. C. Lueth, "Automatic design in MATLAB using PDE toolbox for shape and topology optimization," *Proceedings of the ASME 2019*, 2019.

[27] M. Szilvśi-Nagy, and G. Mátyási, "Analysis of STL Files," *Math. Comput. Model.*, vol 38, pp. 945-950. 2003.

[28] Y. Sun and T. C. Lueth, "Extension of the FEM Analysis Using the PDE-Toolbox of Matlab with Regard to Point Loads, Line Loads, and Freeform Surface Loads: Feature Surface Concept," *Proceedings of 2018 IEEE International Conference on Robotics and Biomimetics (ROBIO)*, pp. 1151–1158,2018.

[29] Y. Sun and T. C. Lueth, "Extension of Matlab' s PDE Toolbox for Developing Bionic Structural Optimization Methods: Overlapping Region Concept," *Advances in Service and Industrial Robotics (Proceedings of RAAD2019)*, pp. 1–8,2019.

[30] J.-P. Kruth, B. Van Der Schueren, J. E. Bonse, and B. Morren, "Basic powder Metallurgical Aspects in Selective Metal Powder Sintering," *Annals of the CIRP*, vol. 45, pp 183-186, 1996.

[31] J. Kruth, X. Wang., T. Laoui, and L. Froyen, "Lasers and Materials in Selective Laser Sintering," *Assembly Automation*, vol. 23, no. 4, pp. 357-371, December 2003.

[32] J. Kruth, P. Mercelis, J. Van Vaerenbergh, L. Froyen, and M. Rombouts, "Binding mechanisms in selective laser sintering and selective laser melting," *Rapid Prototyping Journal*, vol. 11, no. 1, pp. 26-36, 2005

[33] J. Won; K. D. Laurentis; and C. Mavroidis, "Rapid Prototyping of Robotic Systems," *IEEE,* vol. 4, pp. 3077-3082, April 2000.